

Article

# Staircase Recognition and Localization using Convolution Neural Network (CNN) for Cleaning Robot Application

Muhammad Ilyas<sup>1,2</sup>, Anirudh Krishna Lakshmanan<sup>1,3</sup>, Anh Vu Le<sup>1,4</sup> and Mohan Rajesh Elara<sup>1,\*</sup>

<sup>1</sup> Engineering Product Development Pillar, Singapore University of Technology and Design (SUTD), Singapore 487372.

<sup>2</sup> Department of Electrical Engineering, UET Lahore, NWL Campus, Pakistan - 54890.

<sup>3</sup> Department of Computer Science, Birla Institute of Technology and Science (BITS) Pilani, Pilani Campus, Vidyavihar, Rajasthan, India - 333031.

<sup>4</sup> Optoelectronics Research Group, Faculty of Electrical and Electronics Engineering, Ton Duc Thang University, Ho Chi Minh City, Vietnam - 70000.

\* Correspondence: rajeshelara@sutd.edu.sg

**Abstract:** Multi-floor environments are usually ignored while designing an autonomous robot for indoor cleaning applications. However, for efficient operation in such environments, the ability of a robotic platform to traverse staircases is crucial. Staircase recognition and localization is highly important for planning the traversal on staircase by an autonomous robot. This paper describes a deep learning approach using Convolutional Neural Networks (CNNs) based Robot Operation System (ROS) to staircase recognition and localization. We use an object detection network to detect staircases in images. We also localize these staircases using a contour detection algorithm to detect the target point, a point close to the center of the first step, and the angle of approach to the target point. Experiments are performed with data obtained from images captured on different types of staircases at different viewpoints/angles. Results show that the approach is very accurate in identifying the presence of a staircase in the working environment and is also able to locate the target point with reasonable accuracy.

**Keywords:** Staircase recognition, Convolutional Neural Networks (CNN), Re-configurable robot, Contour detection.

## 1. Introduction

Robots are key for automation of various tasks and have revolutionized many fields in the 21<sup>st</sup> century. They are extremely precise and efficient in doing tasks which otherwise would be difficult or impossible. One such type of robots that are becoming increasingly important are cleaning robots, programmed to work in the indoor environments [1–3]. These robots have vast potential to enhance the productivity in cleaning tasks in domestic and commercial settings and have witnessed a steep rise over the last two decades. It is estimated that between 2015 and 2018, about 25.2 million robotic cleaning units would be sold worldwide [4].

Indoor robots are designed for fully autonomous traversal in indoor environments[1]. Typical indoor traversal requires the robot to be able to avoid objects or obstructions by integrating the sensing models and communication modules [5,6]. However, if the environment is multi-floor, the robot is required to have the ability to detect and localize the staircases in order to perform cleaning tasks on the staircase. Conventional indoor cleaning robots are usually designed for single floor operations *i.e* they cannot climb the stairs and reach the next floor. However, many real-world indoor

29 environments have multiple stories connected with staircase. These staircase may be of different types  
30 *e.g.* straight, spiral, L-shaped staircase *etc.* This severely limits the ability of the conventional cleaning  
31 robot to be effective in such scenarios. To enable robots to traverse staircases, accurate detection and  
32 location of staircases are highly critical. This would enable robots to plan and navigate through such  
33 environments, thereby making them much more effective for real-world indoor environments.

34 The problem of recognizing staircase seems straightforward for humans. However, for robots  
35 to be able to detect, recognize and localize the staircases, this task is much more complex. For this,  
36 the robot should be able to analyze the incoming images and detect and recognize stair-like structure  
37 among many others objects. Further, the knowledge of the location of the staircase is required. Also,  
38 knowledge of the angle of approach is required as well for aligning the robot with the staircase in  
39 order to start climbing. This makes staircase detection and localization a highly demanding task for  
40 autonomous robots.

41 In this article, we have designed our solution to work with the sTetro platform [7]. sTetro  
42 is a reconfigurable cleaning robot that can change its shape to climb staircases autonomously. In  
43 previous work, we validated the sTetro robot with respect to area coverage by bench-marking its  
44 performance with a fixed morphology robot. The results indicated that sTetro robot could achieve  
45 superior coverage performance through its shape-shifting ability. However, the validation was done  
46 by passing manual commands to navigate the robot towards the first step position of the staircase,  
47 and there were no autonomous strategies applied. In this paper, we extend our previous works by  
48 integrating the sensing modules and manipulations modules with the sTetro on ROS environment  
49 that enables the robot to navigate autonomously to the staircase. For this, we use a deep learning  
50 approach to detect and recognize staircases in the incoming image stream. However, the robot also  
51 requires knowledge of how to move based on the staircase position/location. So, after detecting  
52 staircases, the next step is to localize the robot with respect to stairs. For this, we use our own contour  
53 detection algorithm to find the target point (center of the first step of the staircase) and angle of  
54 approach. This enables the robot to approach the center of the staircase, align itself to the first stair  
55 and then start climbing.

56 This article is organized as follows: We first discuss related works and other approaches used  
57 for staircase detection. This is followed by details of our proposed approach. Finally, we describe the  
58 experimental setup used to test our approach and the results obtained in this work.

## 59 2. Related Work

60 Many different approaches have been proposed in the literature to address the problem of  
61 staircase detection. These approaches can be grouped based on the sensors and algorithms used.  
62 Standard sensors like RGB and RGB-D have been used for staircase detection, with the prominent  
63 approach being detecting parallel lines in the image [8]. Though this algorithm works for many  
64 scenarios, they have many limitations. Hough transform [9], the preferred approach for detection of  
65 parallel lines, fails to detect staircases which are curved or spiral. Also, these algorithms assume that  
66 the robot is parallel to the staircase and facing it. However, this is not the case for most real-world  
67 scenarios. The robot must be able to detect and then plan their approach to the staircase. These  
68 approaches are also not designed for staircase climbing robots. These robots require alignment with  
69 the staircase which requires data pertaining to the first step of the staircase. Other approaches using  
70 RGB or RGB-D cameras include using Gabor filters, 3D column maps [10] *etc.* These are able to handle  
71 approaching staircases from different angles. Even LiDARs have been used for detection of staircases  
72 [11–13]. However, these approaches also assume that the robot is parallel to the staircase and facing  
73 it. Some other sensors that have been used are monocular [14–17] and stereo sensors [18].

74 Object detection and classification by deep learning CNNs have been researched intensively  
75 over decades and has set revolutionary era in many applications especially in robotics [19,20]. Deep  
76 learning using large neural networks can find the unique features of various objects autonomously,  
77 thereby reducing the need of pre-defined kernel based solutions. Since the features of the objects can

78 be identified, the most significant achievement of these deep learning-based methods is the ability  
 79 to identify uncanny features in object classification. As a result, the effectiveness and accuracy of  
 80 deep learning-based methods outperformed the conventional methods significantly [21]. However,  
 81 the biggest challenge is training these large networks, as they require a large amount of computation  
 82 to converge by estimating the various parameters defined in the network. Recently, technologies  
 83 in parallel computing such as Compute Unified Device Architecture CUDA [22] and NVIDIA  
 84 CUDA Deep Neural Network CuDNN [23], enable parallel computing using multiple threads to  
 85 process large calculations in separate graphics cards with their own Graphics Processing Unit  
 86 (GPU). Consequently, the training time of these networks has reduced sharply. However, deploying  
 87 these deep learning approaches in the compactly embedded controllers is still a big challenge for  
 88 commercial applications. However, with the dawn of IoT devices, using a server-client model to  
 89 reduce this real-time computation load is more practical.

90 There are many advantages to using deep learning for staircase detection. The model can be  
 91 trained to detect different types of staircases including spiral and curved, which prove to be very  
 92 difficult for standard algorithms. Also, they can be trained to recognize staircases from different  
 93 angles. This eliminates the need for the robot to be in front of the staircase. These models are highly  
 94 accurate as well. This is because these models learn the features from data rather specifying them in  
 95 the algorithm. Recently, the advances in object detection, including object localization and objects  
 96 classification, are driven by the success of state-of-the-art convolution network (ConvNet)-based  
 97 object detectors called the Region-based Convolutional Network method (RCNN) [24]. The issue  
 98 with deep learning approaches was the computation power required to run these models in real-time.  
 99 However, with the recent update to MobileNets [25,26] and the release of SSD (Single Shot multi-box  
 100 detectors) [27], these models are now capable of running in real time on low cost hardware. We are  
 101 also computing the target point and the angle of approach, which allows the robot to align itself with  
 102 the center of the staircase, thereby having enough space to be able to climb the staircase.

### 103 3. Methodology

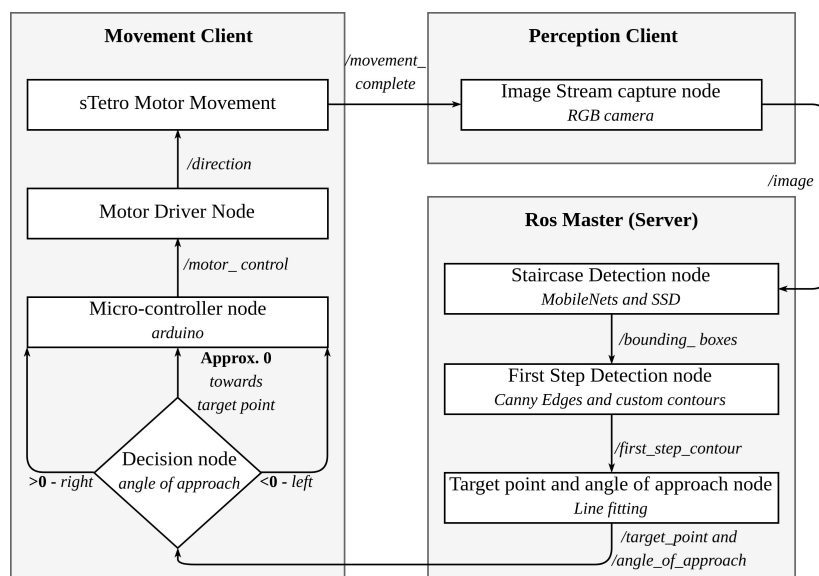


Figure 1. Model Structure

104 Neural networks have large computation costs. Due to this, computing on low powered  
 105 hardware in real-time is almost impossible. Hence, we propose a client-server model for real-time  
 106 applications. The proposed system is built on the ROS platform [28]. ROS provides the infrastructure  
 107 and mechanism for ROS modules. The ROS master installed on remote server monitors the entire

108 ROS system. The ROS-based block diagram of the proposed system using a client- server model  
 109 is shown in Figure 1. The ROS topics transmitted in ROS network through WiFi or data networks  
 110 enable the communication between ROS nodes. Specifically, first, the perception client uses an image  
 111 sensor to extract an image from the image stream and sends it over to the server. The server uses two  
 112 steps to detect and localize staircases. The first step involves detection of staircases. This includes  
 113 extracting features from an RGB image using the MobileNet architectures. We then classify and  
 114 predict a bounding box using the SSD architecture. These rely on the CNN architecture, which is  
 115 explained below. The second step has two components. First, we detect the first step of the staircase.  
 116 The first step information is then used to detect the target point  $p_{x,y}$ , a point close to the center of the  
 117 first step. The angle of approach  $\theta$  is also computed in this step. We then send this information to the  
 118 portion of client responsible for movement. Based on our angle of approach, we decide a movement  
 119 strategy which is executed by the onboard Micro-controller with the help of a motor. While this  
 120 happens, the perception client updates the server on the new data. This is repeated until the target  
 121 point is reached.

### 122 3.1. Convolutional Neural Networks (CNN)

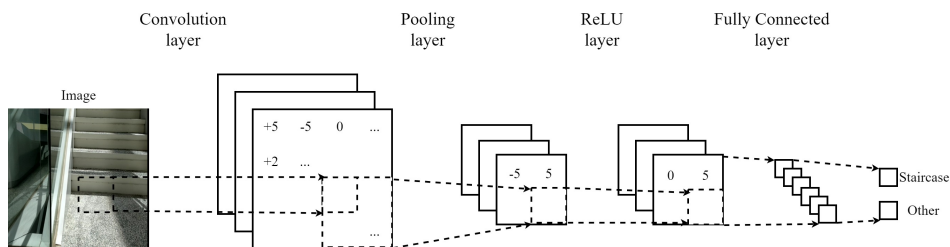


Figure 2. CNN Structure

123 The CNNs are frequently used in image classification due to their high accuracy. Their structure  
 124 is the basis for many object detection and image classification networks, including MobileNets and  
 125 SSD, which we use in our approach. The CNNs consist of four types of layers - Convolution layer,  
 126 Pooling layer, ReLU layer and a Fully Connected layer. The combination of Convolution layer(s)  
 127 and Pooling layer(s) extract features from the image. This is fed to the Fully Connected layer(s) that  
 128 classify the image. Figure 2 shows the structure of a simple CNN.

#### 129 3.1.1. Convolution layer

130 This layer involves applying a filter over the input layer. Typically, multiple filters are applied on  
 131 the input layer. Filters are applied using a sliding window, which slides over the image and applies  
 132 the filter on the region covered by the window. The input layer is zero padded so that the window  
 133 can cover the entire input. The filter used is called the weight function. Equation 1 is used to compute  
 134 the activation function  $f(x)$ .

$$f(x) = w \times x + b \quad (1)$$

135 where  $w$  represents the filter (weights),  $b$  represents the bias and  $x$  represents the input.

#### 136 3.1.2. ReLU layer

137 This layer applies a ReLU function to the input layer. This layer is typically used after the  
 138 Convolution layer. This layer is used to remove the negative values which may have been formed  
 139 from the filter. Equation 2 computes the ReLU activation function  $f(x)$ .

$$f(x) = \max(0, x) \quad (2)$$

140 where  $x$  represents the input layer.

### 141 3.1.3. Pooling layer

142 This layer partitions the input layer into non-overlapping regions on which a pooling function is  
143 applied. Each region outputs a single value. This reduces the dimension of the input while retaining  
144 the important features.

### 145 3.1.4. Fully connected layer

146 This layer is a typical artificial neural network (ANN) layer. It is fully connected to the input  
147 layer. Multiple fully connected layers are used together to classify the image. These are used with the  
148 final pooling layer as input. The final pooling layer represents the extracted features.

## 149 3.2. Feature Extraction using MobileNets

150 Specialized CNN based architectures like MobileNets [25,26], AlexNet [29], Inception [30],  
151 ResNet [31] *etc.* are highly accurate at classifying images. The recently proposed Inception-ResNet  
152 [32] has the highest accuracy. However, we use the MobileNet architecture due to its low computation  
153 cost, which allows for real-time image classification on mobile hardware [33]. Specifically, we use  
154 MobileNetv2 [26], which is an improvement over the standard MobileNet [25]. The basic blocks of  
155 both architectures are shown in Figure 3 and Figure 4. The extracted features of MobileNet is used  
156 by SSD architecture to classify and localize staircases. The structure of SSD is discussed in the next  
157 section.

### 158 3.2.1. MobileNet architecture

159 The core idea behind MobileNet is depth-wise separable convolutions. These replace the  
160 typical convolution layers as computing convolutions are highly expensive. Depth-wise separate  
161 convolutions first apply a depth-wise convolution on the input. This filters the input data. This is  
162 followed by  $1 \times 1$  convolutions which combine these filters into features. These depth-wise separable  
163 layers approximately mimic the function of typical convolution layers but with much faster speed.  
164 Another optimization done was to use ReLU6 instead of ReLU, which applies an upper limit of 6 on  
165 the activation function. Equation 3 is used to compute the activation function  $f(x)$ .

$$f(x) = \min(6, \max(0, x)) \quad (3)$$

where  $x$  is the input. Structure of MobileNet v1 is shown in Figure 3.

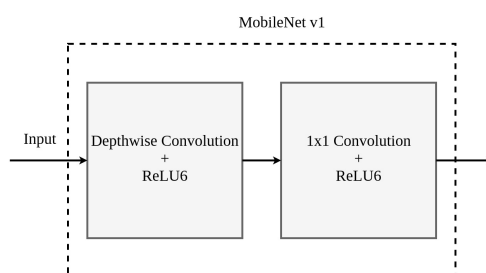


Figure 3. MobileNet v1

166

### 167 3.2.2. MobileNetv2 architecture

168 MobileNet v2 also uses special convolution structures to replace typical convolution layers. First,  
169 there is an expansion layer, which expands the dimension of the input layer tensor. Then the data  
170 is passed through a depth-wise convolution layer. The output of this layer is passed through a

171 projection layer, which adds a linear bottleneck to the tensor. This reduces the dimension of the  
 172 tensor. Structure of MobileNet v2 is shown in Figure 4.

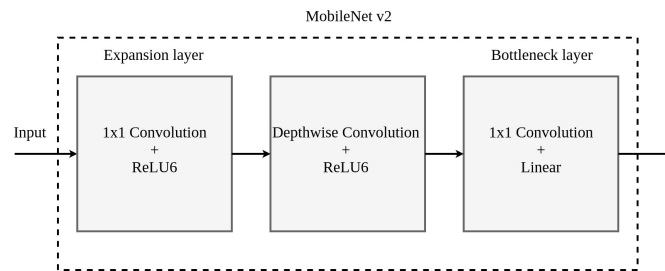


Figure 4. MobileNet v2

172

### 173 3.3. Localization using Single Shot MultiBox Detector (SSD)

174 Though CNN based architectures with fully connected layers can be used to classify images  
 175 and detect staircases, autonomous traversal requires the knowledge of location of staircase as well.  
 176 For this, we need a bounding box over the staircase to calculate its position, which is needed  
 177 for calculating the target point and the angle of approach. For this purpose, object localization  
 178 techniques such as Single Shot Multi-Box Detector (SSD) [27], faster R-CNN [34], YOLO [35] etc.  
 179 can be used. These use the features extracted from CNN based architectures to classify and localize  
 180 objects. Generally, faster R-CNN is the preferred method for object localization due to best accuracy.  
 181 However, SSDs have been shown to perform better in most scenarios for *large objects*, which is the case  
 182 for staircases [33]. SSD is also extremely fast since it requires only one forward pass for computation  
 183 of all bounding boxes. Due to these reasons, SSD is highly appropriate for the current scenario.

#### 184 3.3.1. SSD architecture

185 SSD passes the input through multiple convolution layers. These layers progressively decrease  
 186 in size. Each of these layers generate a fixed set of predictions. This enables predictions of various  
 187 sizes. In addition to this, SSD uses a set of default bounding boxes of different dimensions. These  
 188 are applied to the predictions from different layers, which allows for predictions of boxes of different  
 189 sizes and scales. Although the bounding boxes may not be pixel perfect, the loss in accuracy is found  
 190 to be very minimal. However, due to this, the performance is drastically increased.

#### 191 3.3.2. Loss in SSD training

192 Since SSD involves predicting a bounding box along with the class for an object, typical loss  
 193 computation cannot be followed. Loss in SSD training is a weighted sum of loss due to two aspects -  
 194 confidence and localization. Equation 4 is used for computing total loss  $L$ .

$$L = \frac{1}{N}(L_{conf} + \alpha L_{loc}) \quad (4)$$

195 where  $N$  is the number of matching boxes,  $\alpha$  is the weight term which balances the confidence loss  
 196  $L_{conf}$  and localization loss  $L_{loc}$ . Confidence loss is the loss that occurs due to classification. This is  
 197 computed as Softmax of confidence over multiple classes. Localization loss is the loss in predicting  
 198 the bounding box of the object. This is computed as a smooth  $L_1$  loss between predicted box and  
 199 marked box.

#### 200 3.3.3. Loss optimization

201 We use the Root Mean Square propagation (RMS prop) [36] algorithm to optimize the total loss  
 202 during training. Equations 5, 6, 7 represent the RMS prop algorithm at any time  $t$ .

$$v_t = \beta v_{t-1} + (1 - \beta) g_t^2 \quad (5)$$

$$\Delta w^{rms} = \frac{-\eta}{\sqrt{v_t + \epsilon}} \times g_t \quad (6)$$

$$w_{t+1}^{rms} = w_t^{rms} + \Delta w^{rms} \quad (7)$$

203 where  $g_t$  is the gradient along weight  $w^{rms}$ .  $w_t^{rms}$  is the weight at any time  $t$ .  $v_t$  is the exponential  
 204 average of gradients.  $\eta$  is the initial learning rate.  $\beta$  is a hyperparameter to be tuned.  $\epsilon$  is constant  
 205 with value close to zero to avoid dividing by zero errors.

### 206 3.4. First step detection

207 Through SSD and MobileNets, we are able to detect the staircase and predict a bounding box  
 208 over it. Now, we require knowledge of the first step to determine the target point and angle of  
 209 approach. We do this by analyzing the staircase inside the bounding box. These values enable  
 210 our sTetro robot to move towards the detected staircase autonomously. For detection of steps, the  
 211 prominent method is Hough transform [37], which detects straight lines. However, steps of staircases  
 212 may be curved as well. Traditional contour detection is difficult to handle this situation. Also, we do  
 213 not need to detect all the contours in the image, as we require only the first step in our calculations.  
 214 The proposed method for first step of staircase detection can be divided into two parts. First, we  
 215 detect edges using Canny edge detection, which is followed by contour detection.

#### 216 3.4.1. Edge Detection

217 To be able to detect the first step in the image, we first need to detect edges present in the image.  
 218 For this, we use the Canny Edge detection algorithm [38]. to enhance the accuracy of detected edges,  
 219 the Canny Edge algorithm is divided into 4 steps - Gaussian filters step to remove the noise, gradient  
 220 calculation to find the edge pixel candidates, non-max suppression step to remove the edges with the  
 221 weak gradient responses, hysteresis thresholding step to thin the detected edge lines. This returns a  
 222 edge representation of the image *i.e* only the pixels that constitute edges are positive. Other pixels are  
 223 0.

#### 224 3.4.2. Contour detection algorithm

225 This paper proposes a contour detection algorithm for determining the first step as shown in  
 226 Algorithm 1. The algorithm detects points within a certain distance and certain bounds while giving  
 227 preference to the points along the gradient of the most recent detected points. Before computation, we  
 228 generate *canny*, which is the canny edge representation of the image. We use two functions for this  
 229 algorithm. Function `getContour()` returns the contour representing the first step of the staircase. This  
 230 function uses *canny* to generate a contour representing the first step. It checks the image from bottom  
 231 to top (represented by  $i$ ), left to right (represented by  $j$ ) direction. If an edge point is detected it calls  
 232 `getContourWithIJ()`, with a contour consisting of only the point  $i, j$ . Finally, it returns the contour  
 233 only if its horizontal length is greater than a certain threshold,  $thres_{filter}$ . We set this to 60% of the  
 234 width of the staircase during experiments. This is done using `getBounds()`, which gets the difference  
 235 between horizontal bounds of the contour.

236 Function `getContourWithIJ()` finds the remaining contour from the reference point  $i, j$  in *canny*.  
 237 This is merged with the contour detected prior to this point, which is represented by *contour*. It  
 238 consists of 4 steps to identify the next point in the contour. First, the equation of the line that fits  
 239 the previous 5 points in the contour is generated. The function `fitLine()` does this by line-fitting  
 240 linear regression approach [39]. We also set a bound on the slope of the line. *line* represents this line  
 241 equation. *line.slope* represents the slope of this line. Next, we check all points within a range of  $X$

**Algorithm 1** Contour detection algorithm psuedocode

---

```

1: function GETCONTOUR(canny, thresfilter)
2:   i = canny.length - 1; j = 0
3:   contour = []
4:   while i >= 0 do
5:     while j < canny.width do
6:       contour = GETCONTOURWITHIJ(canny, i, j, contour.append([i, j]))
7:       if getBounds(contour) > thresfilter then return contour
8:       end if
9:       j = j + 1
10:    end while
11:    i = i - 1
12:  end while
13: end function
14: function GETCONTOURWITHIJ(canny, i, j, contour)
15:  arr = empty; t = 0
16:  line = fitLine(contour)
17:  while t < threswidth do
18:    ycoord = line.slope × (t) + i
19:    arr.push(ycoord, j + t, 0)
20:    for item in arr do
21:      bottom = item[0] + item[2]
22:      bottomLimit = item[1] + thres × item[1]
23:      if canny[bottom][item[1]] > 0 and bottom <= bottomLimit then return
        GETCONTOURWITHIJ(canny, bottom, item[1], contour.append([bottom, item[1]))
24:      end if
25:      top = item[0] - item[2]
26:      topLimit = item[1] - thres × item[1]
27:      if canny[top][item[1]] > 0 and top >= topLimit then return
        GETCONTOURWITHIJ(canny, top, item[1], contour.append([top, item[1]))
28:      end if
29:      if top < topLimit and bottom > bottomLimit then
30:        arr.remove(item)
31:      end if
32:      item[2] = item[2] + 1
33:    end for
34:    t = t + 1
35:  end while
36:  while arr.length > 0 do
37:    for item in arr do
38:      bottom = item[0] + item[2]
39:      bottomLimit = item[1] + thres × item[1]
40:      if canny[bottom][item[1]] > 0 and bottom <= bottomLimit then return
        GETCONTOURWITHIJ(canny, bottom, item[1], contour.append([bottom, item[1]))
41:      end if
42:      top = item[0] - item[2]
43:      topLimit = item[1] - thres × item[1]
44:      if canny[top][item[1]] > 0 and top >= topLimit then return
        GETCONTOURWITHIJ(canny, top, item[1], contour.append([top, item[1]))
45:      end if
46:      if top < topLimit and bottom > bottomLimit then
47:        arr.remove(item)
48:      end if
49:      item[2] = item[2] + 1
50:    end for
51:  end while return contour
52: end function

```

---

242 coordinates, represented by variable  $t$ . This variable is bound by a threshold  $thres_{width}$ . Using this,  
243 we compute  $y_{coord}$ , which is the next possible location of the edge. We push this onto an array  $arr$ .  
244 Then, for each element in  $arr$ , we search both above and below the elements. If any of them is part of  
245 an edge, then we call  $getContourWithIJ()$  with the coordinates of this point. If the top and bottom of



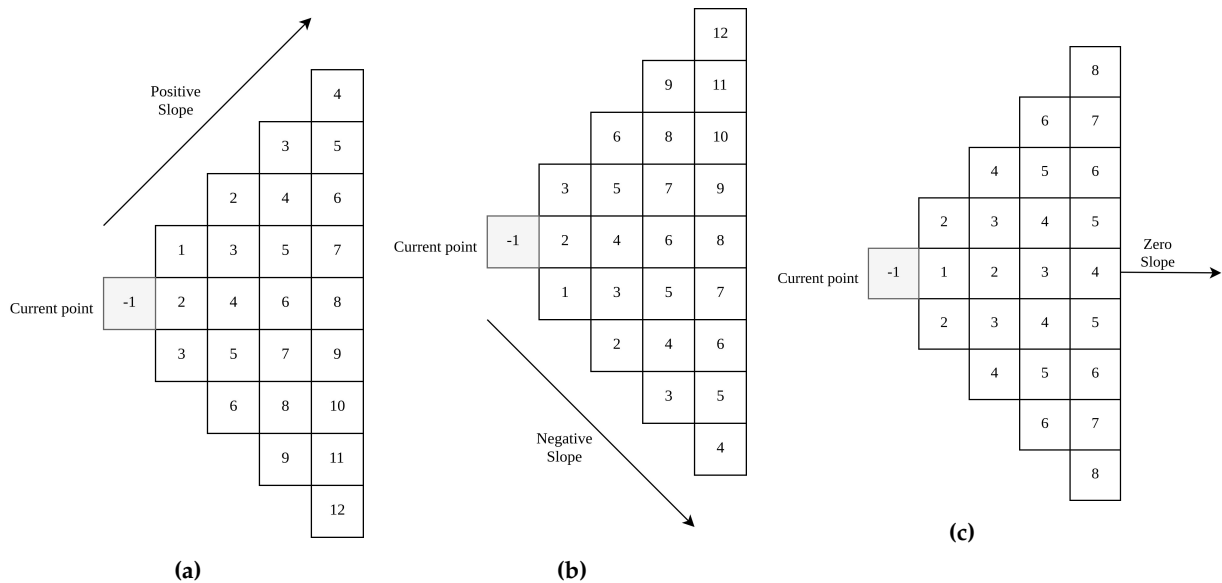


**Figure 5.** Order of evaluation using the contour algorithm. Positive slope ( $+45^\circ$ ) in (a) . Negative slope ( $-45^\circ$ ) in (b) . Zero slope ( $0^\circ$ ) in (c) . The angle of 45 is chosen for easy visualization.

246 this element exists the bound, computed using an angle threshold  $thres$ , the element is removed from  
 247 the array.

248 The working of algorithm for three different scenarios based on slope of *line*, has been shown in  
 249 Figure 5. In this figure, each box represents one pixel in the image. The value in each box represents  
 250 the iteration in which they would be visited. The box with value  $-1$  represents the current pixel on  
 251 which `getContourWithIJ()` is called. The line represents the slope for the given scenario, with the  
 252 value of slope given below each figure. The algorithm clearly gives preference to points along the  
 253 slope while also examining points in the area bounded by  $thres$ . The numbers in boxes represent  
 254 which iteration of algorithm would evaluate those pixels. For two pixels having same iteration  
 255 number, the one which is closest to the slope will be evaluated first.

### 256 3.5. Determining the target point

257 Since we have the contour representing the first step, determining the target point  $p_{x,y}$   
 258 (approximate central position of first step of staircase) is rather simple. We can find  $n$  points which  
 259 are closest to the horizontal center. The distance here is linear distance between the X-coordinates,  
 260 since there would not be multiple points with same X-coordinate. We can then fit a line through  
 261 these points and predict the Y-coordinate of the horizontal center. The horizontal point  $x$  along  
 262 X-coordinate and vertical point  $y$  along Y-coordinate gives the central target point  $p_{x,y}$ . The slope  
 263 of this line is the angle of approach ( $\theta$ ). This is necessary so that the robot can rotate itself to align  
 264 with the staircase. In general, negative angles mean the robot is located to the right of the staircase  
 265 and should rotate clockwise while moving left, so that the robot will become aligned to the staircase.  
 266 Similarly, positive angles mean the robot is located to the left of the staircase and should rotate  
 267 counter-clockwise while moving right. Angles close to zero means the robot is already aligned to  
 268 the staircase. We use a small threshold around zero to accommodate for slight variations, which may  
 269 occur during detection.

## 270 4. Experimental Setup

271 In this section, we discuss about the data-set specification and specification of the models used.  
 272 The data-set was generated by capturing images of different staircases using a RGB camera. Details

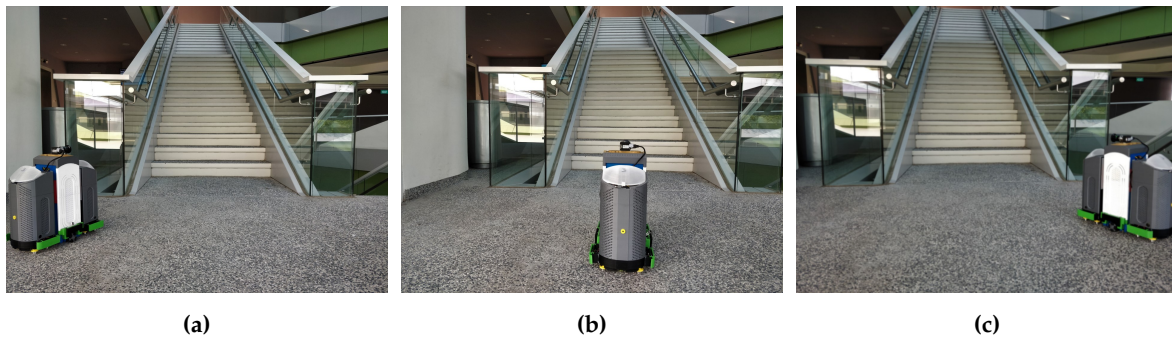


**Figure 6.** sTetro robot capturing images from different angles. (a) left of staircase, (b) in front of staircase, (c) right of staircase.

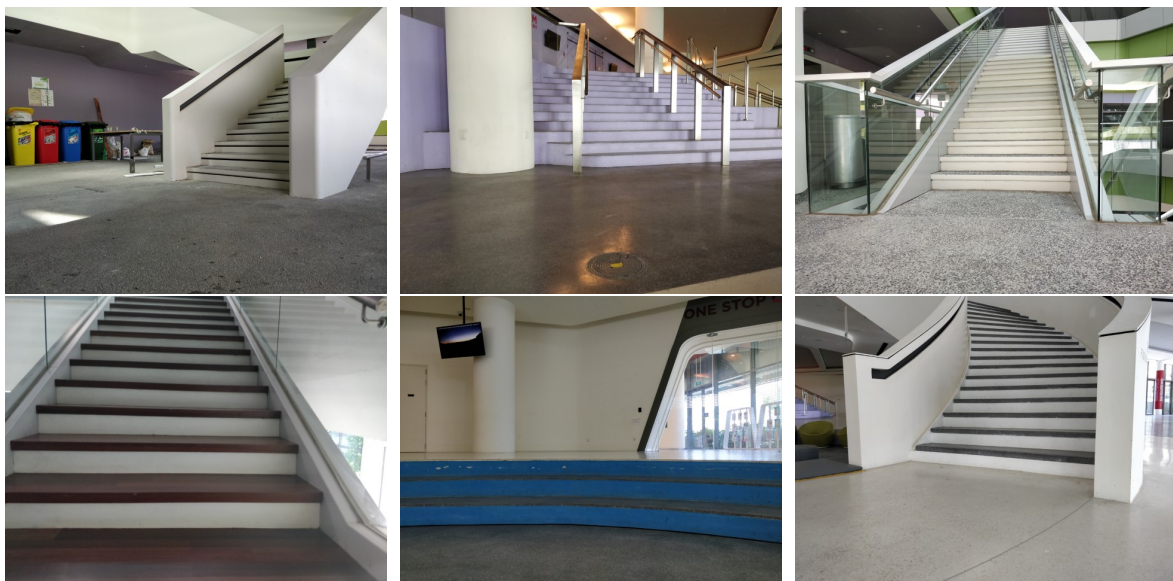


**Figure 7.** Some of the images present in the dataset.

273 of this is discussed below. The weights of the network were initialized to the weights of a network  
 274 trained on the COCO data-set [40], which is a large data-set containing 80 most common classes for  
 275 labelling. This was done so that there would be a faster convergence while training. This also helps  
 276 in achieving a better overall accuracy. We used a batch size of 20 while training. We used a RMS prop  
 277 optimizer for loss optimization with initial learning rate 0.004 and a decay factor of 0.9.

#### 278 4.1. Obtaining Data-set

279 The sTetro robot [7] is used to capture images of the working environment. A RGB camera is  
 280 fitted on top of sTetro robot, which is used to take the images, as shown in Figure 6. Initially the  
 281 images are taken from different staircases at different angles ranging from approximately 0 to 180 in  
 282 front of stairs. Images from different distances and different positions were also taken. All images  
 283 have a resolution  $640 \times 480$  pixels. The data-set consists of 1025 images. The data-set contains images  
 284 of 11 different staircases, which include both straight and curved staircases. Staircases with curved  
 285 steps were also taken. The data-set also has staircases with different materials. A 90 : 10 split was  
 286 taken for training and testing respectively during the training phase. Figure 7 contains some of the  
 287 images present in the data-set.

288 The final results are obtained from a set of 102 images not present in the data-set. Approximately  
 289 half of these images contain staircases in them. The other half includes images of corridors, open areas  
 290 and other common environments for cleaning robots where objects with features similar to staircases  
 291 may be present.

## 292 5. Results Discussion

293 In this section, we discuss about the results obtained on the staircase data-set used. We divide  
 294 this section into two categories: Staircase detection and First step detection.

### 295 5.1. Staircases Detection

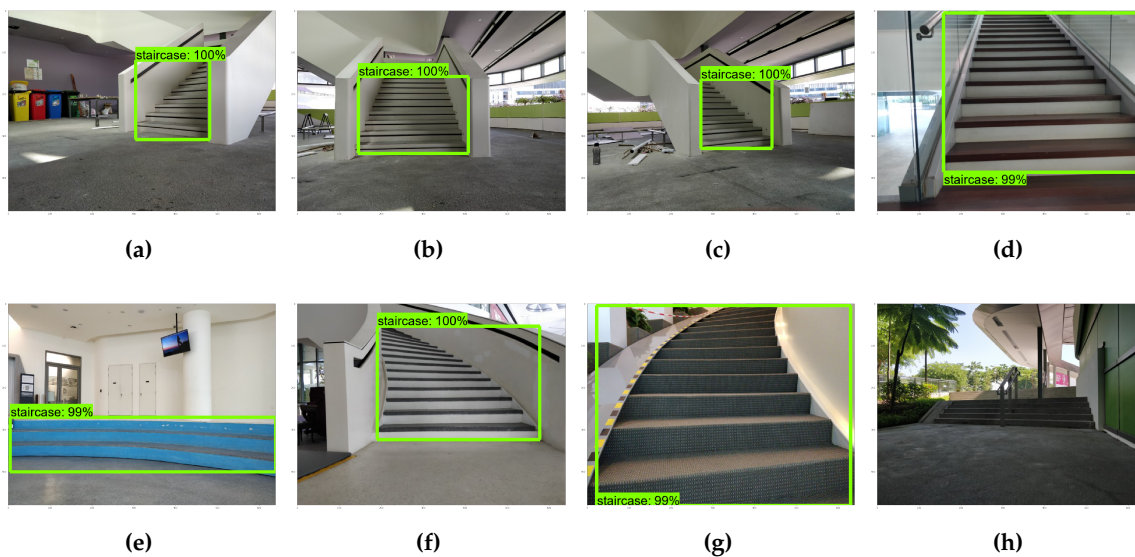
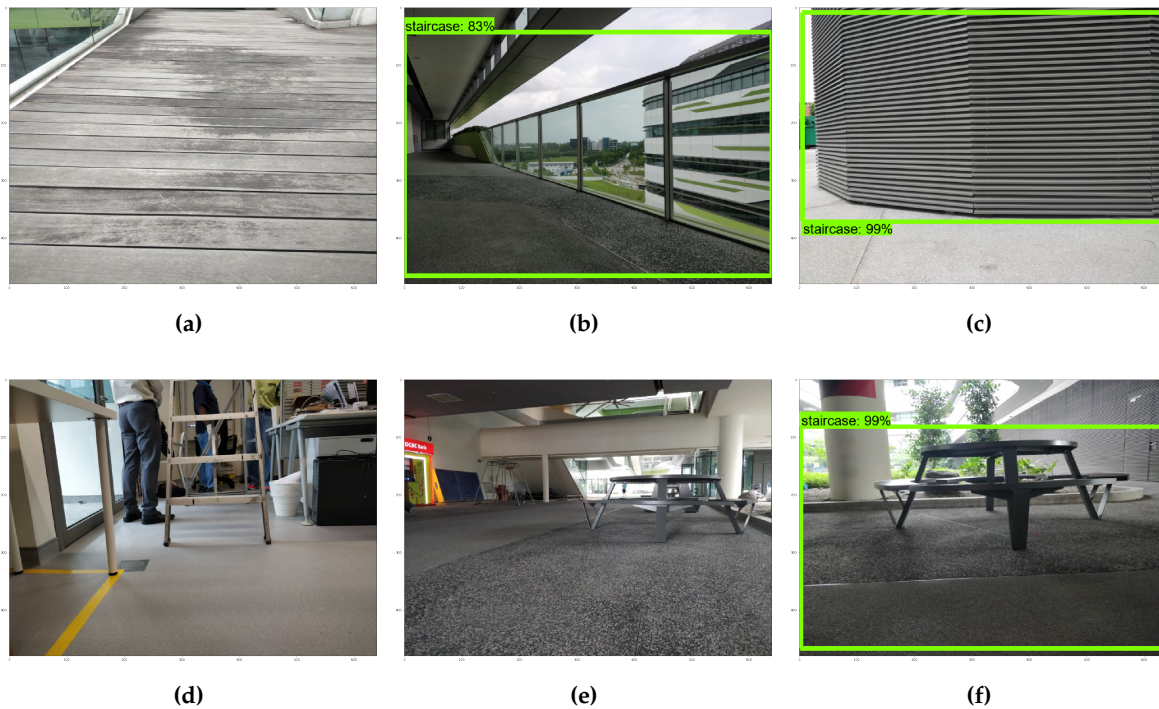


Figure 8. Staircase detection. Staircase detected in (a), (b), (c), (d), (e), (f) and (g). Not detected in (h).

296 This section discusses results pertaining to detection of bounding boxes over staircases. Some  
 297 images of staircases were taken along with images having similar features to staircases. This includes  
 298 structures with parallel lines, ladders, floors with textures *etc.* The model detected almost all staircases  
 299 correctly. This includes different types of staircases and images taken from different angles and  
 300 distances. This is shown in Figure 8. The box represents detected staircase. The confidence of its  
 301 prediction is shown as a percentage above/ below the box. We filter out boxes with confidence less  
 302 than 80% for staircase localization. Figures 8a, 8b and 8c show the model is able to detect staircases  
 303 viewed from different angles. Figure 8d is another staircase with different material. Figure 8e is  
 304 a staircase with curved steps, which the model is able to recognize. Figures 8f and 8g are curved  
 305 staircases with different orientations. The model is able to detect these as well. In Figure 8h, the  
 306 staircase is not detected. This can be attributed to bad lighting conditions and larger distance between  
 307 the robot and the staircase. The model *did not* detect ladders as staircases, which is a common issue  
 308 with traditional methods. Also, the model is able to detect curved staircases, which proves to be a  
 309 challenge for traditional linear line detection based-approaches.

310 However, the model did fail on certain cases where the images were very similar to staircases.  
 311 Some examples of these scenarios are given below in Figure 9. The model is able to differentiate  
 312 between staircases and tiled floors, which have parallel lines. One such example is Figure 9a. This is a  
 313 very common scenario where traditional classifiers struggle, since the floor has parallel lines, which is  
 314 a common feature used to detect staircases. Figure 9b is detected as a staircase. This can be attributed  
 315 to the fact that the railings look like a staircase rotated by 90. However, it is easy to differentiate  
 316 between staircases and railings by considering the angle of lines detected. In Figure 9c, the wall has



**Figure 9.** Negative samples for staircase detection. Staircases are not detected in (a), (d) and (e). False detection in (b), (c) and (f).

317 features similar to a staircase, which causes the model to detect it as a staircase. The model also  
 318 does not detect ladders as staircases. This is shown in Figure 9d. In Figure 9e, the combination of  
 319 table and chair is also not recognized as staircases, although they have similar features. However,  
 320 when combined with lines on the floor, the model detects them as a staircase, as shown in Figure  
 321 9f. However, if we put a constraint on the height of steps *i.e.* a constraint on distance between two  
 322 contour lines, this false detection may be avoided. The overall results are given in Table 1.

**Table 1.** Results of staircase detection.

	Labelled Staircase	Not Detected	Total	Precision (%)
<b>Staircase</b>	42	2	44	95.45
<b>Not Staircase</b>	14	44	58	75.86
<b>Any Image</b>	56	46	102	-

### 323 5.2. First step detection results

324 This section discusses results pertaining to detection of first step of staircases. We use 60% width  
 325 of staircase as the  $thres_{filter}$  to filter out small contours. Also, we filter out all vertical edges by using a  
 326  $thres$  parameter of  $\approx 60^\circ$ . This value is obtained from grid searching through possible values for  $thres$   
 327 and selecting the one with best accuracy. The algorithm is able to detect both the target point  $p_{x,y}$   
 328 and the angle of approach  $\theta$  with good accuracy. The results are showcased in Figure 11. Here, the  
 329 first step of the staircase detected using contour detection is denoted by the line. The cross represents  
 330 the computed target point  $p_{x,y}$ . The detected angle of approach  $\theta$  is also shown below each Figure.  
 331 The algorithm is able to detect these with good accuracy, as shown in Figures 11a, 11b, 11c, 11e, 11f.  
 332 Figure 11d is the image of a textured staircase, where the approach is not very consistent due to the

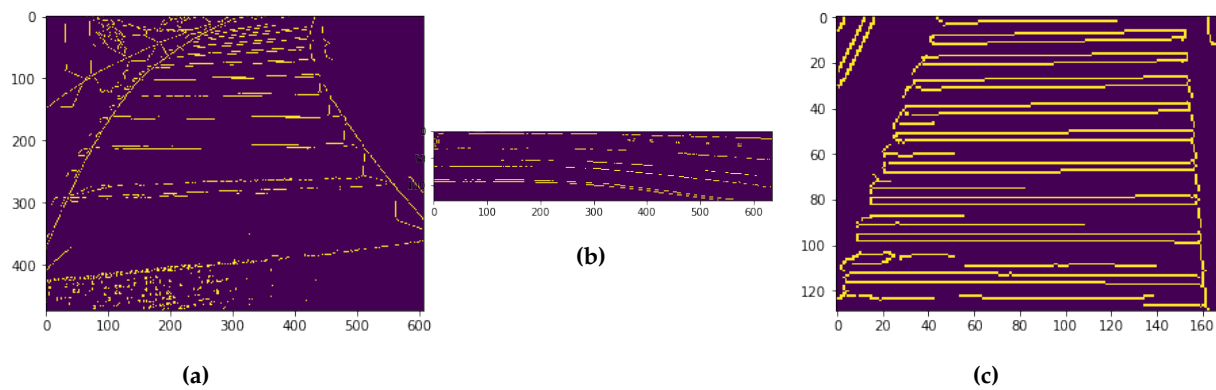


**Figure 10.** Canny edge detection. (a) Noisy edge detection. (b) Curved step edge detection. (c) Straight staircase edge detection.

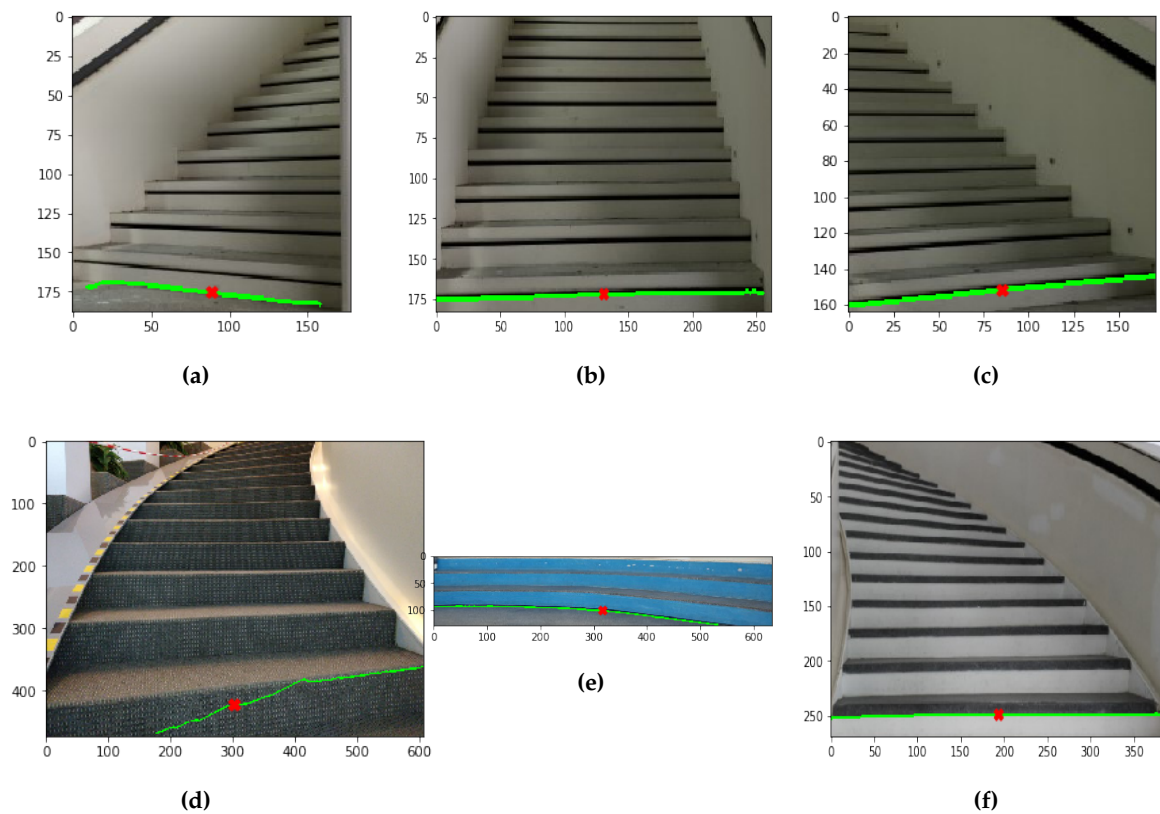


**Figure 11.** First step detection. (a) Detected angle:  $-6.724$ , move left. (b) Detected angle:  $0.678$ , move towards target point. (c) Detected angle:  $5.386$ , move right. (d) Detected angle:  $18.336816$ , move right. (e) Detected angle:  $-4.586$ , move left. (f) Detected angle:  $0$ , move towards target point.

333 noise generated during Canny Edge detection. The edges detected for this image is shown in Figure  
 334 10a. Optimal edge detection results are shown in Figures 10b and 10c.

### 335 5.3. Real-time Performance

336 This section details the real-time tests performed using our proposed model. We used an image  
 337 stream captured from the sTetro robot to determine movement direction in real-time. The robot was

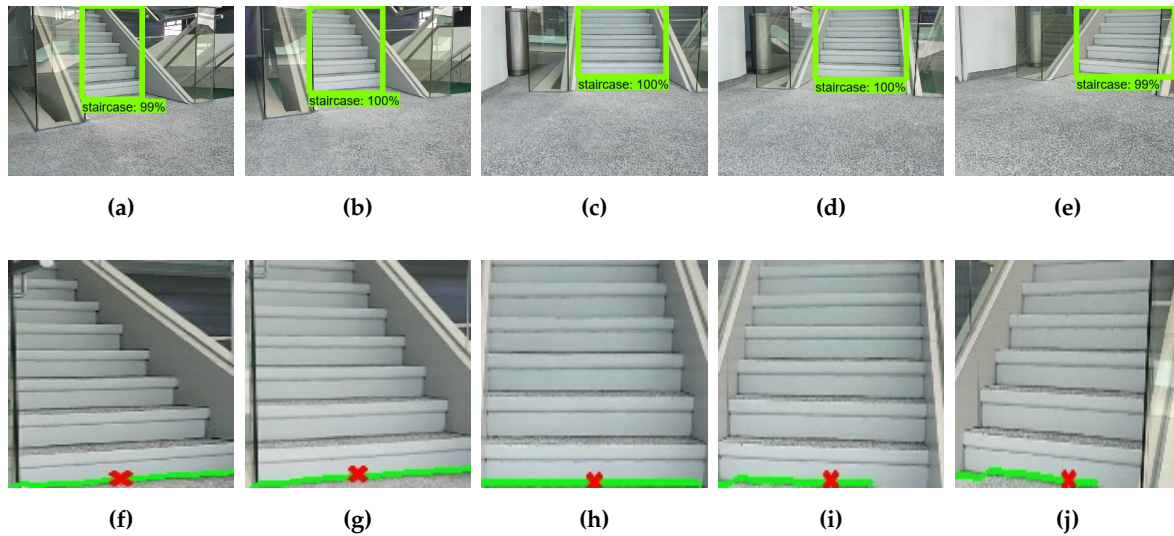


**Figure 12.** Real time staircase detection. (a), (b), (c), (d) and (e) are staircase detection results. (f) is the first step detected in (a) (instruction: move right). (g) is the first step detected in (b) (instruction: move right). (h) is the first step detected in (c) (instruction: move straight). (i) is the first step detected in (d) (instruction: move left). (j) is the first step detected in (e) (instruction: move left).

**Table 2.** Performance of proposed approach. *Times do not include network delays.*

Scenario	Maximum Time(ms)	Average Time(ms)
Staircase Detection	2652	71
First Step Detection	930	83
Total	2684	155

338 able to detect staircases by sending frames after every interval to a server where the server processed  
 339 and returned a direction logic (*i.e* angle of approach) to the robot. Also, the details of the target point  
 340 was sent so that the robot can move towards this location. In this test, the robot is moving from the  
 341 left to the right of staircase. Detection of staircase during this test is shown in Figures 12a, 12b, 12c,  
 342 12d and 12e. The first step detection for these Figures are shown in Figures 12f, 12g, 12h, 12i and 12j  
 343 respectively. The directions predicted are accurate during our testing scenarios, with minor errors  
 344 occurring on textured staircases. The target point is predicted accurately. However, for real-time  
 345 applications, the running time of the algorithm is also crucial. This is given in Table 2. The overall  
 346 approach takes about 150ms on an average, which is feasible for real-time applications. The high  
 347 computation times usually occur during the first run, which can be attributed to the loading of model  
 348 into memory.

## 349 6. Conclusion

350 In this paper, we described an approach to staircase recognition and localization. We first used  
 351 a deep learning model to recognize a staircase in the environment. This was done using an object  
 352 detection network consisting of MobileNet and SSD architectures. We then used canny edge detector  
 353 followed by our own contour detection algorithm for first step detection of staircase. Through this,  
 354 we identified the target point, a point close to the center of the first step and the angle of approach,  
 355 which is used to determine the direction to staircase. This scheme allows to align the robot to the  
 356 staircase, so that it can start traversing the staircase. We trained and tested our proposed model  
 357 using our own data-set consisting of images of 11 different staircases captured with sTetro robot from  
 358 different viewpoints. We also tested our model against images that have features similar to staircases.

359 The model is able to detect staircase and determine the target point and the angle of approach to the  
360 first step of the staircase with good accuracy. We also tested this model for real-time scenarios and  
361 found that it can be used in slow moving platforms like sTetro. In future, this work can be extended  
362 to recognize the type of staircases also, like straight, curved, spiral *etc.* This would allow the robot to  
363 switch between operation modes according to the type of staircase encountered.

## 364 7. Acknowledgement

365 This research was supported by Grant No. RGAST1702 from National Robotics Program  
366 Office, Singapore (NRPO) to the Engineering Product Development (EPD) at Singapore University  
367 of Technology and Design (SUTD).

## 368 References

- 369 1. Prassler, E.; Ritter, A.; Schaeffer, C.; Fiorini, P. A short history of cleaning robots. *Autonomous Robots* **2000**,  
370 9, 211–226.
- 371 2. Jones, J.L.; Mack, N.E.; Nugent, D.M.; Sandin, P.E. Autonomous floor-cleaning robot, 2017. US Patent  
372 App. 15/451,817.
- 373 3. Prabakaran, V.; Elara, M.R.; Pathmakumar, T.; Nansai, S. Floor cleaning robot with reconfigurable  
374 mechanism. *Automation in Construction* **2018**, 91, 155–165.
- 375 4. Choset, H. Coverage for robotics—A survey of recent results. *Annals of mathematics and artificial intelligence*  
376 **2001**, 31, 113–126.
- 377 5. Biswas, J.; Veloso, M. Wifi localization and navigation for autonomous indoor mobile robots. Robotics  
378 and Automation (ICRA), 2010 IEEE International Conference on. IEEE, 2010, pp. 4379–4384.
- 379 6. Huang, A.S.; Bachrach, A.; Henry, P.; Krainin, M.; Maturana, D.; Fox, D.; Roy, N. Visual odometry and  
380 mapping for autonomous flight using an RGB-D camera. In *Robotics Research*; Springer, 2017; pp. 235–252.
- 381 7. Ilyas, M.; Yuyao, S.; Elara, M.R.; Devarassu, M.; Kalimuthu, M. Design of sTetro: A Modular,  
382 Reconfigurable and Autonomous Staircase Cleaning Robot. *Journal Of Sensors* (in press).
- 383 8. Munoz, R.; Rong, X.; Tian, Y. Depth-aware indoor staircase detection and recognition for the visually  
384 impaired. Multimedia & Expo Workshops (ICMEW), 2016 IEEE International Conference on. IEEE, 2016,  
385 pp. 1–6.
- 386 9. Duda, R.O.; Hart, P.E. Use of the Hough transformation to detect lines and curves in pictures.  
387 *Communications of the ACM* **1972**, 15, 11–15.
- 388 10. Sinha, A.; Papadakis, P.; Elara, M.R. A staircase detection method for 3D point clouds. Control  
389 Automation Robotics & Vision (ICARCV), 2014 13th International Conference on. IEEE, 2014, pp.  
390 652–656.
- 391 11. Oßwald, S.; Hornung, A.; Bennewitz, M. Improved proposals for highly accurate localization using  
392 range and vision data. Intelligent Robots and Systems (IROS), 2012 IEEE/RSJ International Conference  
393 on. IEEE, 2012, pp. 1809–1814.
- 394 12. Johnson, A.M.; Hale, M.T.; Haynes, G.; Koditschek, D.E. Autonomous legged hill and stairwell ascent.  
395 Safety, Security, and Rescue Robotics (SSRR), 2011 IEEE International Symposium on. IEEE, 2011, pp.  
396 134–142.
- 397 13. Mihankhah, E.; Kalantari, A.; Aboosaeedan, E.; Taghirad, H.D.; Ali, S.; Moosavian, A. Autonomous  
398 staircase detection and stair climbing for a tracked mobile robot using fuzzy controller. Robotics and  
399 Biomimetics, 2008. ROBIO 2008. IEEE International Conference on. IEEE, 2009, pp. 1980–1985.
- 400 14. Hernández, D.C.; Jo, K.H. Stairway tracking based on automatic target selection using directional filters.  
401 Frontiers of Computer Vision (FCV), 2011 17th Korea-Japan Joint Workshop on. IEEE, 2011, pp. 1–6.
- 402 15. Cong, Y.; Li, X.; Liu, J.; Tang, Y. A stairway detection algorithm based on vision for ugv stair climbing.  
403 Networking, Sensing and Control, 2008. ICNSC 2008. IEEE International Conference on. IEEE, 2008, pp.  
404 1806–1811.
- 405 16. Se, S.; Brady, M. Vision-based detection of staircases. Fourth Asian Conference on Computer Vision  
406 ACCV, 2000, Vol. 1, pp. 535–540.

- 407 17. Hesch, J.A.; Mariottini, G.L.; Roumeliotis, S.I. Descending-stair detection, approach, and traversal with  
408 an autonomous tracked vehicle. *Intelligent Robots and Systems (IROS), 2010 IEEE/RSJ International*  
409 *Conference on. IEEE, 2010, pp. 5525–5531.*
- 410 18. Lu, X.; Manduchi, R. Detection and localization of curbs and stairways using stereo vision. *Robotics and*  
411 *Automation, 2005. ICRA 2005. Proceedings of the 2005 IEEE International Conference on. IEEE, 2005, pp.*  
412 *4648–4654.*
- 413 19. LeCun, Y.; Bengio, Y.; Hinton, G. Deep learning. *nature* **2015**, *521*, 436.
- 414 20. Schmidhuber, J. Deep learning in neural networks: An overview. *Neural networks* **2015**, *61*, 85–117.
- 415 21. Ji, S.; Xu, W.; Yang, M.; Yu, K. 3D convolutional neural networks for human action recognition. *IEEE*  
416 *transactions on pattern analysis and machine intelligence* **2013**, *35*, 221–231.
- 417 22. Weninger, F.; Bergmann, J.; Schuller, B. Introducing currennt: The munich open-source cuda recurrent  
418 neural network toolkit. *The Journal of Machine Learning Research* **2015**, *16*, 547–551.
- 419 23. Chetlur, S.; Woolley, C.; Vandermersch, P.; Cohen, J.; Tran, J.; Catanzaro, B.; Shelhamer, E. cudnn: Efficient  
420 primitives for deep learning. *arXiv preprint arXiv:1410.0759* **2014**.
- 421 24. Girshick, R.; Donahue, J.; Darrell, T.; Malik, J. Region-based convolutional networks for accurate object  
422 detection and segmentation. *IEEE transactions on pattern analysis and machine intelligence* **2016**, *38*, 142–158.
- 423 25. Howard, A.G.; Zhu, M.; Chen, B.; Kalenichenko, D.; Wang, W.; Weyand, T.; Andreetto, M.; Adam,  
424 H. Mobilenets: Efficient convolutional neural networks for mobile vision applications. *arXiv preprint*  
425 *arXiv:1704.04861* **2017**.
- 426 26. Sandler, M.; Howard, A.; Zhu, M.; Zhmoginov, A.; Chen, L.C. Inverted Residuals and Linear Bottlenecks:  
427 Mobile Networks for Classification, Detection and Segmentation. *arXiv preprint arXiv:1801.04381* **2018**.
- 428 27. Liu, W.; Anguelov, D.; Erhan, D.; Szegedy, C.; Reed, S.; Fu, C.Y.; Berg, A.C. Ssd: Single shot multibox  
429 detector. *European conference on computer vision. Springer, 2016, pp. 21–37.*
- 430 28. Quigley, M.; Conley, K.; Gerkey, B.; Faust, J.; Foote, T.; Leibs, J.; Wheeler, R.; Ng, A.Y. ROS: an open-source  
431 Robot Operating System. *ICRA workshop on open source software. Kobe, Japan, 2009, Vol. 3, p. 5.*
- 432 29. Krizhevsky, A.; Sutskever, I.; Hinton, G.E. Imagenet classification with deep convolutional neural  
433 networks. *Advances in neural information processing systems, 2012, pp. 1097–1105.*
- 434 30. Szegedy, C.; Vanhoucke, V.; Ioffe, S.; Shlens, J.; Wojna, Z. Rethinking the inception architecture for  
435 computer vision. *Proceedings of the IEEE Conference on Computer Vision and Pattern Recognition,*  
436 *2016, pp. 2818–2826.*
- 437 31. He, K.; Zhang, X.; Ren, S.; Sun, J. Deep residual learning for image recognition. *Proceedings of the IEEE*  
438 *conference on computer vision and pattern recognition, 2016, pp. 770–778.*
- 439 32. Szegedy, C.; Ioffe, S.; Vanhoucke, V.; Alemi, A.A. Inception-v4, inception-resnet and the impact of residual  
440 connections on learning. *AAAI, 2017, Vol. 4, p. 12.*
- 441 33. Huang, J.; Rathod, V.; Sun, C.; Zhu, M.; Korattikara, A.; Fathi, A.; Fischer, I.; Wojna, Z.; Song, Y.;  
442 Guadarrama, S.; others. Speed/accuracy trade-offs for modern convolutional object detectors. *IEEE*  
443 *CVPR, 2017.*
- 444 34. Ren, S.; He, K.; Girshick, R.; Sun, J. Faster r-cnn: Towards real-time object detection with region proposal  
445 networks. *Advances in neural information processing systems, 2015, pp. 91–99.*
- 446 35. Redmon, J.; Divvala, S.; Girshick, R.; Farhadi, A. You only look once: Unified, real-time object detection.  
447 *Proceedings of the IEEE conference on computer vision and pattern recognition, 2016, pp. 779–788.*
- 448 36. Tieleman, T.; Hinton, G. Lecture 6.5-RMSProp, COURSE: Neural networks for machine learning.  
449 *University of Toronto, Technical Report* **2012**.
- 450 37. Ballard, D.H. Generalizing the Hough transform to detect arbitrary shapes. *Pattern recognition* **1981**,  
451 *13*, 111–122.
- 452 38. Canny, J. A computational approach to edge detection. *IEEE Transactions on pattern analysis and machine*  
453 *intelligence* **1986**, pp. 679–698.
- 454 39. Edwards, A.L. *An introduction to linear regression and correlation*; WH Freeman San Francisco, 1976.
- 455 40. MS COCO dataset. <http://cocodataset.org/#home>. Accessed: 2018-07-05.